POLITECNICO
MILANO 1863

SCUOLA DI INGEGNERIA INDUSTRIALE
E DELL'INFORMAZIONE

Executive Summary of the Thesis

Novel Techniques for Actuator Line Modelling of Floating Offshore Wind Turbines

Laurea Magistrale in Energy Engineering - Ingegneria Energetica

Author: Agnese Firpo

Advisor: Giacomo Bruno Azzurro Persico

Co-advisors: Andrea Giuseppe Sanvito, Paolo Schito

Academic year: 2021-2022

1. Introduction

Floating Offshore Wind Turbines (FOWTs) may experience large platform motions producing complicated aerodynamic phenomena. Currently, the development of a fast computational model for studying the unsteady aerodynamic is one of the most important research objects. To this end, an Actuator Line Model (ALM) is adopted. By substituting the blades with volume forces, the model combines the high accuracy of a CFD analysis with a consistent reduction in calculation times. In the ALM, blades are reproduced through a series of actuator points, each of them consisting in a source force application using the aerodynamic coefficients provided by the airfoil polars. To this end, the key point is the correct definition of the local attack angles (AoA) and relative velocities, computed by extracting directly velocity components from the flow field. The aim of this research is to propose and validate three new velocity sampling methods needed to provide an accurate AoA and thus blade loads, even in case of FOWT motions. The goal is to sample the real velocity on the blades, excluding the bound circulation effect associated to lift production. The velocity is sampled close to the AL point, where the body-force is applied, but far enough from the point itself not to be affected by numeric oscillations and disturbances. Sampling directly on the AL point is possible but, the huge velocity gradient around it would generate problems of interpolation and numerical stability. A thorough comparison with the experiments is provided and used to evaluate the reliability of the techniques implemented.

2. Experimental Set-Up

Two experimental campaigns are available for the validation phase, both carried out at the Galleria del Vento Politecnico di Milano in the frame of the UNAFLOW (Exp.1) and OC6 (Exp.2) research projects. The test turbine is a 1:75 scaled version of the DTU 10-MW RWT. The experimental campaigns imply one tested case in fixed-bottom condition and a set of surge and pitch platform motions. The fixed-bottom case (LC1.1) is performed at a fixed rotational speed of 240 rpm and a free-stream velocity of 4 m/s (both kept constant for all the cases). The platform motions are applied as imposed sinusoidal laws:

$$x_s(t) = A_s sin(2\pi f_s t + \Phi_s) \quad (1)$$

$$\theta_p(t) = A_p \sin(2\pi f_p t + \Phi_p) \quad (2)$$

Subscripts s and p stand for surge or pitch. The surge simulation is conducted with the turbine moving forward (negative x, with Φ_s= 180°), conversely in the pitch motion it starts moving backward (positive x). The difference in speed between the hub velocity, produced by the platform motion, and the free stream wind U_∞ is the apparent wind experienced by the rotor (Fig.1). In this work, two unsteady cases are studied: surge (LC2.5) with a surge amplitude of 0.035 m and a frequency of 1.0 Hz; pitch (LC3.5) with a pitch amplitude of 1.4° and a frequency of 1.0 Hz.

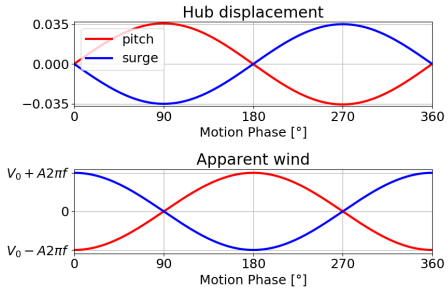

Figure 1: Hub displacement and apparent wind in the surge and pitch case.

3. Actuator Line model

The ALM was introduced by Sørensen at al. [4]. In this work, the ALM model is implemented in the open source OpenFoam, as extension of an original in-house code proposed by Shito et al [3]. The local absolute velocity $\mathbf{U}$=(U_{ax}, U_{tg}) is extracted directly from the resolved CFD flow field, according to the selected velocity sampling strategy. The relative velocity, attack angle (α) and the Reynolds number are computed as:

$$U_{rel} = \sqrt{U_{ax}^2 + (\Omega r + U_{tg})^2} \quad (3)$$

$$\alpha = \arctan\left(\frac{U_{ax}}{\Omega r + U_{tg}}\right) - \gamma, \quad Re = \frac{\rho U_{rel} c}{\mu} \quad (4)$$

Where γ is the local pitch angle. From the AoA and Re number, the lift and drag forces, per unit length, are computed and used to obtain the overall force $\boldsymbol{f}$ that is then smoothly distributed on several mesh points to avoid singular behavior. Thus, a spreading function η_{ker} is applied taking the convolution of the previous force. Finally this force is inserted in the Navier Stokes equations as a source term (Eq. 6).

$$\boldsymbol{f_\epsilon} = \boldsymbol{f} \otimes \eta_{\mathbf{ker}}, \quad \eta_{\mathbf{ker}} = \frac{1}{\epsilon^2 \pi} exp[-(d/\epsilon)^2] \quad (5)$$

$$\frac{\partial \boldsymbol{U}}{\partial t} + \boldsymbol{U} \cdot \boldsymbol{\nabla U} = -\boldsymbol{\nabla} p + \nu \boldsymbol{\nabla}^2 \boldsymbol{U} + \boldsymbol{f_\epsilon} \quad (6)$$

In this thesis, the 2D Gaussian smearing function η_{ker} (Eq. 5) is adopted being more accurate in reproducing the sharp end of the blade at the tip. The value of the smearing factor over average cell size, ϵ/Δ, is set to 2 as suggested by [5], as a compromise between numerical stability and reliable turbine power prediction. This model is able to properly simulate the detachment of the tip vortex, thus inherently capturing the induced drag, but the consequent reduction of force, along the span, is not perceived since a tip losses factor is not included.

4. CFD numerical set-up

The unsteady nature of the FOWT physics requires an Unsteady Reynolds Averaged Navier-Stokes (URANS) formulation with k-ω SST turbulence model. The code only models the turbine blades, including neither the tower nor the nacelle. The discretized domain size is set following the physical dimensions of the wind tunnel and requiring to have the external patches far enough to not artificially influence the flow field. Two refinement regions are introduced to improve the resolution in the rotor and the wake regions, achieving a cell size Δ=0.017 m. The overall numerical domain is a Cartesian grid with 11.4 million cells (Fig.2).

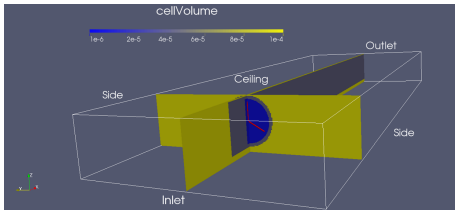

Figure 2: Numerical domain.

In this work, the mesh refinement is defined respecting specific values of some main parameters ($\frac{\epsilon}{D}$, $\frac{\epsilon}{c}$) suggested by literature, to ensure accuracy in power prediction. Furthermore, the final refinement mesh level is the result of some attempts, done on different sampling strategies, that required to limit the mesh refinement to control the number of AL points, as better described in Sec.5. Thus, the final mesh is the result between a proper number of AL points, a proper accuracy in power prediction and an acceptable computational burden.

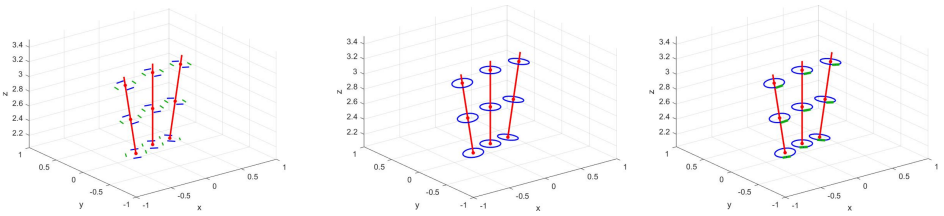

(a) Lines (b) Circle (c) Vortex

Figure 3: Sampling techniques in pitch case.

5. Velocity sampling methods

Line sampling method: the aim is to demonstrate that a simple and easy to implement sampling criterion can still prove valid. The sampled velocity must be already devoid of the bound vortex local effect, to directly compute the correct AoA. This method samples speeds on four lines: U_{ax} is sampled on an upstream and downstream line, both perpendicular to the relative velocity, and then averaged between the two; U_{tg} is sampled in the same way but on lines parallel to the relative velocity. The lines are 10Δ distant from the AL point and 8Δ long. They are constructed on the plane perpendicular to the blade axis using rigid body motion transformation matrix. In Fig.3(a) the sampling lines are shown for three sections in case of pitch motion, only for the vertical blade. The green lines are parallel to the relative velocity and sample U_{tg} while the blue ones are perpendicular and sample U_{ax}.

The distance and length have been decided after a detailed analysis performed using different positions of the lines. From the resolution of the difficulties encountered, the optimal parameters of the line sampling geometry were defined. Here, only the two most significant attempts are cited. These two trials sample the velocities exactly on the same lines of the "Line sapling method" but with different distance (d) and length (l) and on a mesh containing a further refinement region around the rotor ($\Delta_{ref}=\Delta/2$). Since tested in the fixed-bottom case, they are called LC11_mRef_a and LC11_mRef_b. In particular $d_a=4\Delta_{ref}$, $l_a=4\Delta_{ref}$, $d_b=10\Delta_{ref}$, $l_b=8\Delta_{ref}$. Fig.4 shows the sampled axial and tangential velocities along the blade, averaged over the last revolution period. Nonphysical oscillations are visible when: 1) the sampling is too close to the AL point where strong velocity gradients are present, producing instability and interpolation problems; 2) the sampling is performed on an excessively refined mesh so that the number of AL points (intersections between mesh and actuator line) is greater than typical values suggested in literature, producing over-fitting with consequent numerical instabilities. The removal of the additional level of refinement and the greater distance of the lines (LC11_lines) led to the elimination of these oscillations and to the final configuration of the mesh and of the line sampling method.

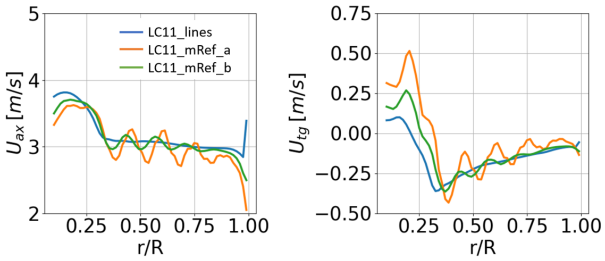

Figure 4: Sampled speeds along the blade span.

Circle sampling method: it arises from a more physical motivation related to how the bound vortex acts on the flow field and how its effect can be removed by velocity sampling. The method samples on a circle centered in the AL point. The induced velocities at opposite points of the circle simplify each other by eliminating the influence of bound circulation. The velocity components are sampled at 36 points along the circle and then averaged. The circle radius is 10Δ to compare the results with the previous method (Fig.3(b)).

Vortex sampling method: The bound circulation around the airfoil section is represented by a concentrated point vortex centered in the AL point. The velocity is sampled on a line upstream and perpendicular to the relative velocity

and then corrected by subtracting the induced one. To compute the circulation and the induced speed, a circle centered on the AL point is once again defined. The bound vortex is computed using the Kutta-Joukowski law; then the induced velocity is obtained using Biot-Savart law; the effective velocity is calculated at the sampling points on the line, by subtracting the induced velocity from the sampled one and then an average is applied. The line is 10Δ upstream and 8Δ long while the circle has 36 points at a 10Δ radius (Fig.3(c)).

6. Fixed-bottom case

The new sampling techniques are validated in the fixed-bottom case with experiments and computational results of other OC6 participants. OC6 is an international research project with the aim to validate and compare academic in-house codes for the analysis of loads acting on a FOWT under both steady and unsteady operating conditions. The Politecnico di Milano took place through the realization of the experimental campaign and the validation of the original in-house code.

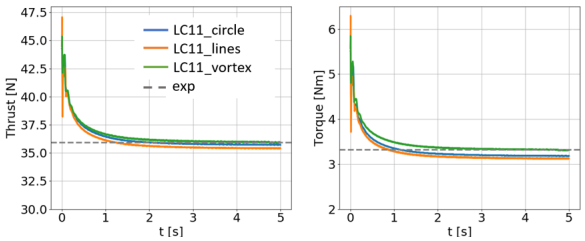

Figure 5: Thrust and torque convergence.

Fig.5 shows the integral quantities versus the simulated time. 5 seconds (corresponding to 20 revolutions) are enough to reach a good convergence. The grey dashed line is the experimental mean value. The new methods present a uniform trend in time, demonstrating their good stability. Since the tower is not simulated and the flow is uniform, there is no reason to have thrust and torque variations during the single revolution.

	EXP	*lines*	*circle*	*vortex*
Thrust	35.91 N	-1.39%	-0.52%	+0.06%
Torque	3.32 Nm	-5.72%	-4.22%	-0.3%

Table 1: Errors versus experimental data.

The final mean values, obtained as average over the last 5 revolutions, are compared with those of the experiment (Tab.1). The errors are all lower than 6%, in particular they are very limited for the *vortex* method. These results can be considered very good, being definitely within the uncertainty band of the experimental data. To assess if the numerical outcomes have a physical meaning, the blade-distributed quantities are analyzed, starting from the comparison of U_{ax} and U_{tg} span-wise distributions between the new sampling techniques (Fig.6).

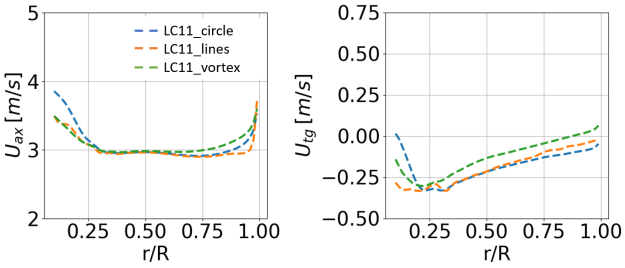

Figure 6: Sampled velocities at 60 stations.

The tangential component is not thoroughly studied because its weight is minimal in computing the AoA. U_{ax} lower than the free stream (4 m/s) proves that all the three methods are correctly estimating an induction effect. The main differences are located at the root and at the tip. At the root the blade aerodynamics is not adequately simulated because the highly 3D flow and separation are not properly captured when boundary layer is not resolved. At the tip, all methods sample a lower flow deceleration (increasing U_{ax}), consistent with the steep drop in forces caused by the chord reduction (tip losses effect on force is not simulated), demonstrating their good validity. In this region, the U_{ax} differences are due to the different nature of the techniques applied. Blade span experimental quantities are not available so, the validation is performed using results from some of the OC6 participants. The institutes considered with the correspondent methods are: DTU (Technical University of Denmark) with a CFD+Vortex Filament; NREL (National Renewable Energy Laboratory) with a Blade Element Momentum method; UNIFI (Università degli Studi di Firenze) with an Actuator Line Model; USTUTT (University of Stuttgart) with a fully-resolved CFD. Fig.7 shows the comparison for some relevant quantities and proves a

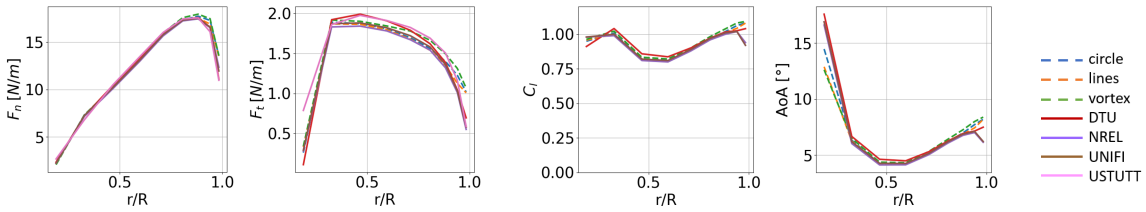

Figure 7: LC1.1 case: spanwise distributed quantities. Comparison with OC6 results [2] [1] .

good agreement with the other participants. At the tip the new normal and tangential force, the lift coefficient and the AoA are higher than those of other institutes due to the lack of tip losses coefficient in the actual techniques. The implementation of a loss coefficient, should promote a stronger drop of the forces at the tip and a corresponding reduction of C_l. Conversely, the effect of tip loss insertion on the AoA is more complex to predict due to the 3D flow. Differences in the AoA are visible also at the root where the flow detachment and the trailing vorticity affect the sampling strategy reducing the AL accuracy. However, this region has a very limited effect on the global turbine performance so it does not affect the overall accuracy of the model.

7. Surge platform motion case

The validation is performed through a comparison with experiments and OC6 participants. Fig.8 shows thrust and torque evolution over a complete surge period T_{surge}= 1 s, including also the OC6 simulations previously described. The maximum and minimum thrust and torque are obtained in correspondence of the maximum and minimum apparent velocity (Fig.1).

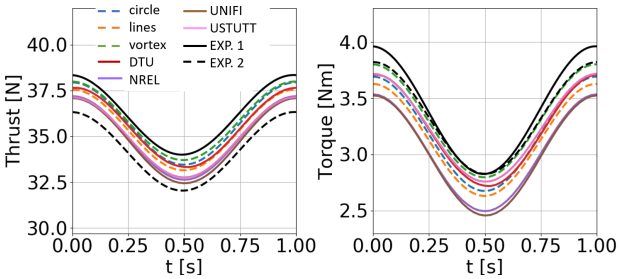

Figure 8: Thrust and torque over a surge period compared with other OC6 participants [2] [1].

At $\frac{1}{4}T_{surge}$ and $\frac{3}{4}T_{surge}$ the rotor is at the two extremes with a null translation velocity, so the fixed-bottom case quantities are reached, indicating that the surge frequency and amplitude, do not change the mean operation with respect to a fixed-bottom condition. The mean and amplitude values of thrust and torque are computed for a quantitative comparison with measurements, demonstrating a good agreement for both thrust and torque. Regarding the thrust, all the three new methods give results included between the two test campaigns. Indeed, the percentage errors are within -2.5% and +5%, proving the great validity of the new techniques in surge case. As far as torque, the three proposed numerical simulations are in better agreement with Exp.2 for both mean and amplitude torque, with errors within -6% and +0.7%. The comparison with OC6 simulations shows that all the participants achieved coherent values, much closer to Exp.2 (Fig.9).

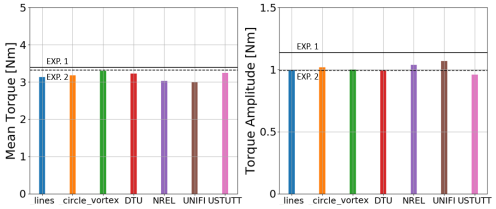

Figure 9: Mean torque and toque amplitude. Comparison with other OC6 participants [2] [1].

Therefore, the origin of the discrepancy with Exp.1 has to be searched in a measurement error and not in a lack of the proposed methods. As a consequence, the difference from Exp.1 does not reduce the validity of the proposed methods in surge case.

8. Pitch platform motion case

For the validation phase in pitch motion, Exp.2 is used, as well as the OC6 results of the institutes already adopted. Fig.10 shows thrust and torque evolution over a complete pitch period T_{pitch}= 1 s. As before, the maximum and min-

imum thrust and torque correctly correspond to the maximum and minimum apparent velocity (Fig.1), while the fixed-bottom case quantities are reached in the extremes ($\frac{1}{4}T_{pitch}$ and $\frac{3}{4}T_{pitch}$).

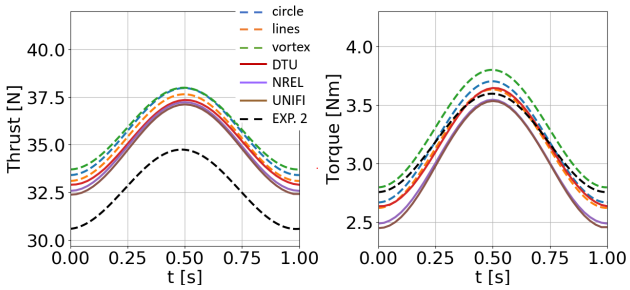

Figure 10: Thrust and torque over a pitch period compared with other OC6 participants [2] [1].

Again the mean and amplitude values of thrust and torque are compared with measurements. An overall good consistency with experiments is obtained for both thrust and torque. For the thrust amplitude and mean torque, the errors, for the three strategies, are all within -1.6% and +3.75%. The greater errors are those computed for the mean thrust and for the torque amplitude. For these quantities a further verification is performed using the OC6 results (Fig.11).

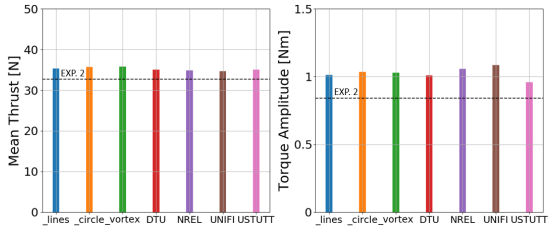

Figure 11: Mean thrust and torque amplitude. Comparison with other OC6 participants [2] [1].

All the simulations overestimate the mean thrust and the torque amplitude if compared to the Exp.2. Taking this observation into account, although the new strategies have errors of the order of +9% on the mean thrust and of +6% on the torque amplitude, with respect to Exp.2, they are considered acceptable. This allows to confirm their validity even in the pitch motion case.

9. Conclusions

Three new sampling strategies of the velocity perceived by the rotor have been implemented, in an already available in-house code, to allow a more accurate estimation of the attack angle and to make the model more flexible and better applicable to unsteady motion conditions. The work proves that the new models enable to estimate reliable velocity with physical spanwise trend coherent with the force distribution. In both fixed-bottom and unsteady conditions, they show a good agreement with the experimental data and when results tend to deviate from these, however, excellent coherence with other OC6 outputs is found, as a further confirmation. Although all the three methods show valid results, the circle and the vortex ones are considered the most interesting as based on physical considerations. Between the two techniques, the vortex strategy seems to be the most promising being more innovative than what is currently available in literature. Future developments include: a more specific sensitivity analysis on the geometrical parameters of the sampling methods, simulations of more extreme surge and pitch cases to verify the good reproduction of more complex aerodynamics; implementation of a tip losses model; wake analysis (using large eddy simulation). The improved ALM could represent a promising tool for studying the wakes interaction in wind farms and for developing new algorithms or new artificial intelligence techniques for control strategies.

References

[1] Atmosphere to Electrons (A2e). oc6/oc6.phase3. Maintained by A2e Data Archive and Portal for U.S. Department of Energy, Office of Energy Efficiency and Renewable Energy. Accessed: 16 03 2023.

[2] Amy Robertson. Oc6 phase iii: Validation of wind turbine aerodynamic loading during surge/pitch motion.

[3] P Schito and A Zasso. Actuator forces in cfd: Rans and les modeling in openfoam. In *Journal of Physics: Conference Series*, volume 524, page 012160. IOP Publishing, 2014.

[4] Jens Norkær Sorensen and Wen Zhong Shen. Numerical modeling of wind turbine wakes. *J. Fluids Eng.*, 124(2):393–399, 2002.

[5] Niels Troldborg. Actuator line modeling of wind turbine wakes. 2009.